Unbiased phosphoproteomic method identifies the initial effects of a methacrylic acid copolymer on macrophages

Michael Dean Chamberlain[a,1], Laura A. Wells[a,1,2], Alexandra Lisovsky[a], Hongbo Guo[b], Ruth Isserlin[b], Ilana Talior-Volodarsky[a], Redouan Mahou[a], Andrew Emili[b], and Michael V. Sefton[a,c,3]

[a]Institute of Biomaterials and Biomedical Engineering, University of Toronto, Toronto, ON, Canada M5S 3G9; [b]Donnelly Centre for Cellular and Biomolecular Research, University of Toronto, Toronto, ON, Canada M5S 3G9; and [c]Department of Chemical Engineering and Applied Chemistry, University of Toronto, Toronto, ON, Canada M5S 3G9

Edited by Robert Langer, Massachusetts Institute of Technology, Cambridge, MA, and approved July 21, 2015 (received for review May 5, 2015)

An unbiased phosphoproteomic method was used to identify biomaterial-associated changes in the phosphorylation patterns of macrophage-like cells. The phosphorylation differences between differentiated THP1 (dTHP1) cells treated for 10, 20, or 30 min with a vascular regenerative methacrylic acid (MAA) copolymer or a control methyl methacrylate (MM) copolymer were determined by MS. There were 1,470 peptides (corresponding to 729 proteins) that were differentially phosphorylated in dTHP1 cells treated with the two materials with a greater cellular response to MAA treatment. In addition to identifying pathways (such as integrin signaling and cytoskeletal arrangement) that are well known to change with cell–material interaction, previously unidentified pathways, such as apoptosis and mRNA splicing, were also discovered.

phosphoproteomic | material–cell interactions | macrophage | methacrylic acid

A conventional description of the interaction between cells and a material begins with protein adsorption (as affected by material chemistry or topography) that translates into the resulting effects on cell adhesion, migration, proliferation, or differentiation (1–3). This perspective is driven by the goal of understanding biocompatibility (4) or of creating scaffolds for tissue engineering. However, the complexity of these interactions limits the ability to understand and control the biological responses to biomaterials, perhaps underscoring the occasional failure of devices in the clinic (5). Furthermore, the metrics of the conventional approach are often disconnected in time scale from the cellular response. Proteins adsorb in seconds, cell behavior changes in hours, and biocompatibility is determined in days and weeks. The materials are agonists of the biological response, whether it is an inflammatory response (6) or cell differentiation (7, 8), but assays that focus on a particular time scale or pathway risk missing the key determinants. The present study focuses on the molecular changes that occur within 30 min of cell exposure to a material, to identify the cell processes that happen between recognition of protein adsorption and adaptation of the cell.

When cells contact a material (via adsorbed proteins), surface receptors are activated and downstream signaling cascades are initiated. The activation of each receptor results in the initiation of multiple signaling cascades that direct the biological response of the cells to the material. Signaling cascades typically involve kinases and phosphatases that change the phosphorylation patterns of proteins to regulate downstream behaviors such as apoptosis, gene expression, cytoskeletal rearrangement, and differentiation. We hypothesized that the manner in which a material influences cell responses may be inferred by studying changes in the phosphorylation events of the intracellular signaling cascades (Fig. 1*A*). This work used phosphoproteomics to detect, in an unbiased manner, actively phosphorylated proteins in cells exposed to two different materials to identify novel interactions. Ultimately, we see the potential to develop "rules of engagement" between cells and biomaterials.

This study investigated the effects of a methacrylic acid (MAA) copolymer on cells because these polymers have been shown to promote vascular regenerative responses in vivo (9, 10), but the mechanism behind this response is unknown (11–13). Previous studies showed that 45% poly(MAA-co-methyl methacrylate [MM]) copolymer beads promoted vascularization and improved wound healing in diabetic mice (10) or with skin grafts in rats (9). In vitro MAA beads altered the gene-expression pattern in macrophage-differentiated THP1 cells (dTHP1) over 4 d (11). Recently, smooth copolymer films of isodecyl acrylate (IDA) and MAA, or IDA and MM as a control, were studied (Fig. 1*B*); MAA films resulted in increased gene expression of IL-6, IL-1β, TNF-α, HIF-1α, and SDF-1α and decreased expression of osteopontin in dTHP1 cells (13), consistent with the previous bead work.

Phosphorylation Changed with Time and Polymer Type

The dTHP1 cells were grown on porous transwell inserts and exposed to 40% MAA-co-IDA or 40% MM-co-IDA films by placing polymer-coated coverslips on top of a monolayer of cells for 10, 20, or 30 min (Fig. 1*C*). The transwell insert allowed for nutrient and oxygen exchange between the cells and the medium while in contact with the material; there were no obvious changes in cell morphology, as expected. After incubation with the materials, the cells were lysed in urea buffer and the proteins

Significance

Cells interact with materials, such as those used in implants, through an adsorbed protein layer that causes changes in cell behavior and gene expression. We have identified the activation of signaling pathways in the cell by a material by unbiased screening of changes in phosphorylation patterns in the cell after material exposure to the material. These changes were apparent 10 min after exposure, filling the gap between the seconds of protein adsorption and the hours of gene expression and leading to the identification of hitherto unknown effects of materials on cells.

Author contributions: M.D.C., L.A.W., A.L., and M.V.S. designed research; M.D.C., L.A.W., A. L., H.G., I.T.-V., and R.M. performed research; M.D.C., L.A.W., A.L., H.G., and R.I. analyzed data; and M.D.C., L.A.W., A.L., A.E., and M.V.S. wrote the paper.

The authors declare no conflict of interest.

This article is a PNAS Direct Submission.

[1]M.D.C. and L.A.W. contributed equally to this work.

[2]Present address: Department of Chemical Engineering, Queen's University, Kingston, ON, Canada K7L 3N6.

[3]To whom correspondence should be addressed. Email: michael.sefton@utoronto.ca.

This article contains supporting information online at www.pnas.org/lookup/suppl/doi:10.1073/pnas.1508826112/-/DCSupplemental.

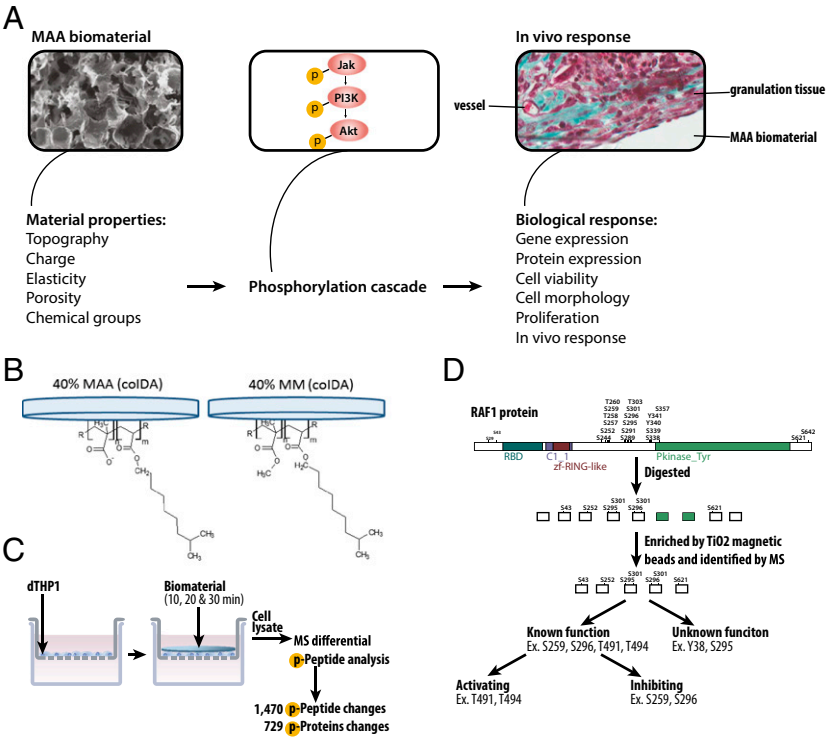

Fig. 1. Overview of phosphoproteomic method to assess the effects of materials on biological responses. (*A*) Biological responses (e.g., gene expression, cell proliferation, in vivo host response) are related to material properties (e.g., topography or chemistry) through phosphorylation signaling cascades. The properties of the material govern how proteins from the extracellular milieu adsorb to the surface of the biomaterial and are presented to the cell. These proteins activate the signaling phosphorylation cascades within the cell that drive the biological response to the material. (*B*) Films containing MAA or MM copolymerized with IDA were cast onto the underside of glass coverslips. (*C*) Coverslips coated with 40% MAA or 40% MM films were placed on serum-starved dTHP1 cells for 10, 20, or 30 min (with films lying atop cells in a Transwell insert), after which the cells were lysed with urea buffer. The cell lysate was digested with trypsin and the phosphorylated peptides were enriched from the cell lysate by TiO_2 magnetic beads and analyzed by MS. (*D*) Phosphorylated peptides from proteins (RAF-1 is shown as an example) were enriched and identified by MS. Peptides were sorted based on the function of the phosphorylation site. Some proteins had a known function of the phosphorylation site that was further distinguished by literature review; other phosphorylation sites had no known function.

digested with trypsin. The phosphopeptides were enriched from the total peptide mixture by TiO_2 magnetic beads and identified by using an Orbitrap Velos mass spectrometer coupled with separation via an inline nano-HPLC (14).

Peptide lists were generated from the MS data by using MaxQuant (Dataset S1), and unphosphorylated peptides were removed and equivalent peptides were combined, generating a list of 1,470 peptides (Dataset S1) corresponding to 729 proteins (Dataset S2). At each time point, there were a greater number of peptides and proteins that were uniquely present in cells exposed to MAA compared with MM (Fig. 2*A*). In addition to the several hundred peptides that were phosphorylated in cells treated with either material at each time point (overlap in Venn diagrams in Fig. 2*B*), there were also hundreds that were uniquely phosphorylated with each material treatment, showing that there are large differences in the cell response to the two materials. Although phosphorylation does not necessary correlate to protein or cell activity, the higher number of phosphorylated peptides in cells exposed to MAA suggests that MAA might have generated more changes in the dTHP1 cell signaling machinery. Furthermore, there was also a change in the phosphorylation pattern over time for each material treatment, showing that the cells response was dynamic (Fig. 2*C*).

In cells exposed to MAA or MM, phosphorylation occurred mostly at serine groups (~85%), with fewer phosphorylations at threonine groups (~14%) and the least number of phosphorylations at tyrosine groups (~1%; Fig. S1); these are the expected percentages (15, 16) and validate the TiO_2 column as an unbiased method for the enrichment of phosphopeptides. In general, there were three types of phosphorylations that were identified in this screen: (*i*) phosphorylations that are known to promote the activity of the protein, (*ii*) phosphorylations that are known to inhibit the activity of the protein, and (*iii*) phosphorylations that have, as yet, no known function (Fig. 1*D*).

Global Trends in Protein Phosphorylation

To visualize the data and to identify global trends, phosphorylated proteins were tested for pathway enrichment by using the Database for Annotation, Visualization, and Integrated Discovery (DAVID) (17, 18). Enrichment results were visualized in Cytoscape 3.1 (19) using the enrichment map application (20) whereby nodes represent pathways and edges represent the gene overlaps, or cross-talk, between pathways [calculated using $P < 0.05$, false discovery rate (FDR) < 0.1, and Jaccard coefficient cutoff of 0.25], which links pathways that share a large proportion of genes and helps reduce the redundancy that exists in pathway databases. Fig. 3 illustrates the cellular processes and pathways that had an increase in protein phosphorylation at 10 min after cell exposure to 40% MAA or 40% MM. In the 10-min data, there were four large clusters of nodes (Fig. 3, red circles), indicating that dTHP1 cells exposure to MAA increased the phosphorylation of proteins involved in cell death and apoptosis, RNA splicing, signaling, and chromosome rearrangement. In addition, there are individual nodes that were unique to MAA treatment (Fig. 3, red circles) that show MAA also caused changes in cytoskeleton rearrangement, endocytosis, and

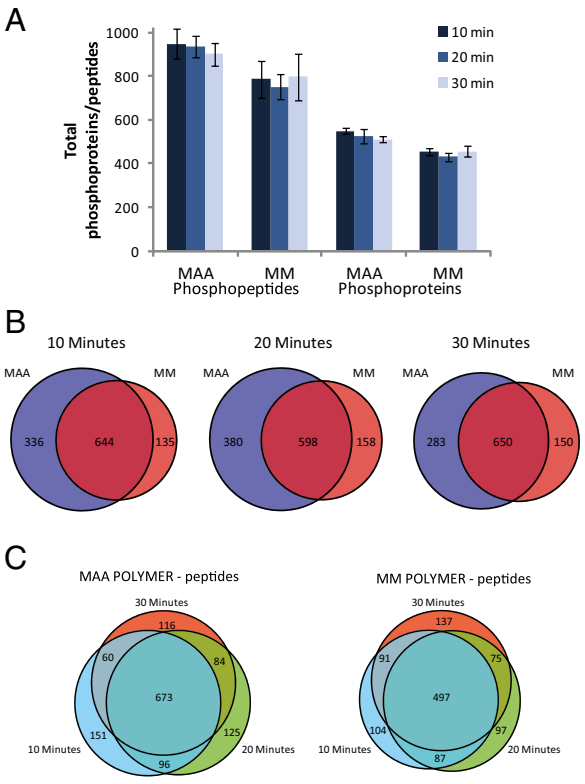

Fig. 2. Landscape of identified phosphorylated peptides and proteins. (*A*) The number of peptides (*Left*) identified via MS and the number of corresponding proteins (*Right*) from which the peptides came. The bars represent the time (10, 20, 30 min) the cells were exposed to the material. (*B*) Venn diagrams illustrating the overlap or difference in phosphorylation of peptides in the cells treated with MAA (blue) or MM (red). There are a large number of phosphorylated peptides present in both MAA- and MM-treated cells at each time point, but there were also many phosphorylated peptides present only with exposure to only MAA or only MM; these peptides are the unique phosphorylation events. (*C*) Change in phosphorylated peptide profile over time for cells treated with each material. Cells exposed to either material had a large number of phosphorylated peptides that were present at all times, but each also had many phosphorylated peptides that were present at only one or two time points.

signaling pathways. The MM material-treated cells had fewer unique nodes in the enrichment map, and these nodes were involved in cell migration and signaling events. In general, there were fewer unique changes in the enrichment maps at 20 and 30 min (Fig. S2). An alternative pathway analysis protocol using Kyoto Encyclopedia of Genes and Genomes (KEGG) identified similar pathways as the enrichment map analysis (Dataset S3).

When cells contact materials, their surface receptors and membrane proteins are the first to respond to the material and its adsorbed proteins. There were 51 phosphorylated surface proteins, including cytokine and growth factor receptors, integrins, transporters, and ADAMs (Dataset S4). Across all time points, the MAA treatment caused the phosphorylation of more surface proteins than the exposure to the MM material, and MAA-treated cells had more uniquely phosphorylated surface proteins (Fig. 4*A*). These surface proteins most likely initiated the intracellular signaling cascades identified by MS that result in the downstream biological responses observed in previous studies (11, 13).

After activation of the surface receptors (by MAA or MM), there is transduction of the signal from the membrane to the interior of the cell, with phosphorylation (via kinases) or dephosphorylation (by phosphatases) being a prominent feature of changes in signaling cascades. The targeted search of the database determined that there were 69 kinases and phosphatases that were phosphorylated in cells exposed to MM or MAA (Dataset S5), and, again, there were more uniquely phosphorylated kinases and phosphatases with MAA treatment (Fig. 4*B*).

Signaling cascades often result in a change in the activation state of transcription factors that drive specific gene expression programs within cells. This causes altered protein expression levels, which lead to adaptation of the cell behavior to a new environment (i.e., the presence of MAA or MM). Transcriptional regulation was identified by the enrichment map, which contained several nodes of Gene Ontology (GO) terms relating to chromatin rearrangement and modification, which are major events in transcriptional regulation. Additionally, a manual screen identified 41 transcription factors (or associated proteins) that were phosphorylated with exposure to either material (Dataset S6). At every time point, there were more transcription factors uniquely phosphorylated in cells with MAA treatment than with MM treatment (Fig. 4*C*).

Together, these results form a picture of what is going on in the cell after exposure to the biomaterials, even as early as 10 min after contact, and allow for identification of the initial mechanisms of interaction that result in biological responses of cells to the MAA material. This method detected phosphorylation changes in pathways that lead to short-term and long-term adaptations, but it also identified "intermediate-term" modifications that adapt the cell to the material quickly without changing gene expression (Fig. 5). For example, multiple proteins involved in translation, RNA stability, and mRNA splicing were differentially phosphorylated, showing that there are significant changes in posttranscriptional regulation of the cell with MAA exposure. These modifications involve cellular activities that are not typically studied in the biomaterials field. In general, biomaterial experiments measure cell morphology changes, such as attachment or cytoskeleton rearrangement, or long-term adaptation of the cells to the material by measuring changes in gene expression. This shows the importance of an unbiased screen to identify novel signaling pathways.

Changes in Protein Phosphorylation at the Local Level

In addition to global differences observed in cells treated with MAA or MM, a detailed analysis of each protein and how its phosphorylation affects protein function (i.e., activating or inhibiting) yielded additional insights. Sample analyses of particular proteins are used to illustrate this local perspective.

There were a large number of surface proteins that were differentially phosphorylated. Some membrane proteins, such as solute transporters or plasma membrane calcium-transporting ATPase 4 (AT2B4), may mediate rapid changes for the cell. For example, the solute transporter monocarboxylate transporter 4, which is involved in lactate secretion (21), was phosphorylated with MAA exposure, although the functional consequence of this particular phosphorylation site is unknown. Lactate is produced to a higher level in "M1" macrophages, and its secretion promotes angiogenesis (16, 21). Integrins are important mediators of cell responses, and integrin A4 and integrin A5 were differentially phosphorylated with MAA or MM treatment, but the function of these differentially phosphorylated sites are unknown. However, there were downstream differences in the integrin signaling cascades with material exposure. Integrin-linked kinase-associated serine/threonine phosphatase (ILKAP) was phosphorylated only in MAA-treated cells, suggesting that the difference in phosphorylation patterns of integrin A4 and A5 did have downstream consequences.

Integrins link to the cytoskeleton, and both the enrichment map and KEGG pathway analysis identified the cytoskeleton as a node of interest. There were many phosphorylated actin and microtubule cytoskeletal proteins with both materials. For example, ARC1b, which is part of the Arp2/3 complex that controls

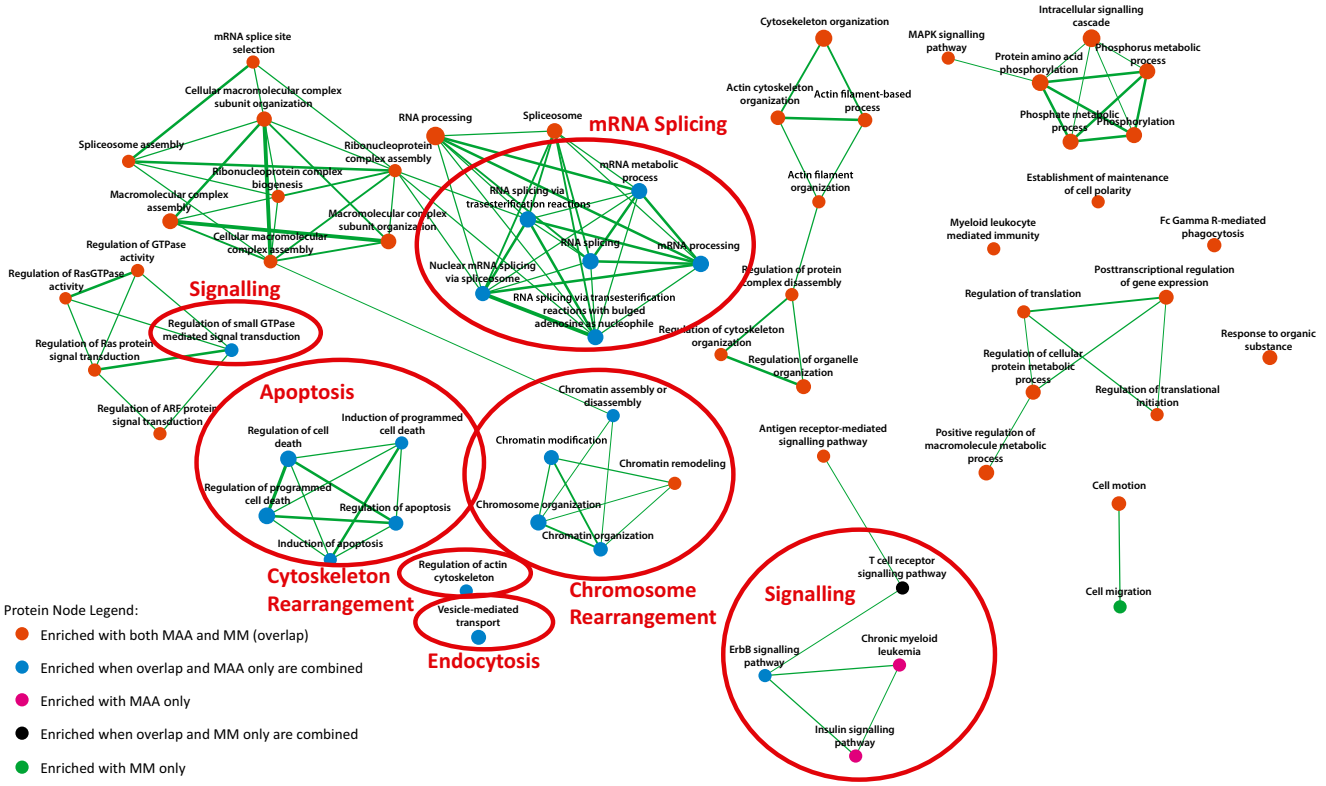

Fig. 3. Enrichment map of the phosphoproteomic data showing phosphorylated proteins identified by MS at 10 min generated with the enrichment map application (filtered with $P < 0.5$, FDR < 0.1, Jaccard coefficient > 0.25) by Cytoscape 3.1. Each node represents several proteins with the same GO or pathway term. Node size is correlated to the number of proteins found in the GO term or pathway. Edges represent the gene overlaps, or cross-talk, between pathways, and the width of the line indicates the strength of the gene overlap. Color coding was used to distinguish among different subsets of identified proteins; e.g., orange shows the proteins that were found in cells treated with either material (derived from the 644-peptide overlap as per Fig. 2), whereas blue shows the proteins that were in the overlap region combined with those that were found only with MAA treatment (derived from the additional 336 peptides unique to MAA at 10 min).

nucleation of actin polymerization and branching of filaments (22), was phosphorylated with MAA treatment. In MM-treated cells, serine 138 of BCL10 was phosphorylated at 10 and 20 min, whereas, in MAA-treated cells, it was phosphorylated only at 20 min. BCL10 affects actin polymerization and phagocytosis (23). Microtubule dynamics were also altered with MAA treatment, as the tubulin-binding proteins MAP1B and CKAP5, microtubule-associated serine/threonine kinase 2 (MAST2), and dynein heavy-chain 14 were phosphorylated. In further support of these actin and microtubule differences, there were different phosphorylation patterns of focal adhesion and ruffling proteins. Fascin, which may promote pseudopod extensions (i.e., ruffling) (24), was phosphorylated at 30 min in MAA-treated cells. At the same time, paxillin, a focal adhesion protein (25), was phosphorylated only in MM-treated cells. This suggests that the cells attach differently to MAA than MM through focal adhesions, and then extend pseudopods (i.e., ruffling) with MAA treatment, resulting in increased contact with MAA in comparison with MM. dTHP1 cells had increased adherence and viability on MAA films in comparison with MM films (13), supporting the notion that MAA and MM treatment have different effects on dTHP1 cell adhesion-related interaction.

The enrichment map (Fig. 3) showed a large cluster of nodes related to cell stress and apoptosis for cells exposed to MAA. This was interesting because MAA materials were not suspected to affect these pathways. The data here suggest that MAA may be antiapoptotic. For example, in cells exposed to MAA, BAD was phosphorylated in cells at S118, which inhibits apoptosis (26); Bcl6 corepressor (BCOR), which reduces apoptosis by inhibiting apoptosis-inducing protein Bcl6 (27), was also phosphorylated; and 4EBP1, a protein that is known to be involved in apoptosis via cell stress and the mTOR pathway (28), was differentially phosphorylated at S94 (but with unknown effect). Bcl-2–associated transcription factor 1 (BCLAF1) was differentially phosphorylated with material treatment, but the function of these phosphorylations is unknown. This unexpected effect on apoptosis was confirmed by showing that the activity of caspase 3 caused by serum starvation of dTHP1 cells was reduced in cells exposed to MAA (Fig. S3). Furthermore, several heat-shock proteins, which modulate cell stress response, were also differentially phosphorylated. Heat-shock protein 105 kDa (HSp105) was differentially phosphorylated at s809 (unknown effect) at early time points (10 and 20 min) in MAA-treated dTHP1 cells. HSp105 is involved in blocking aggregation of unfolded proteins via interactions with HSP70 and has been shown to reduce stress-induced apoptosis (29). Conversely, cell interaction with MM materials may promote apoptosis to some degree, as PEA-15 was phosphorylated at s116, which stabilizes this death domain-containing protein (30).

Interestingly, there were DNA damage proteins that were phosphorylated when the cells were incubated with MAA. This was unexpected but may be explained by recent work showing that some DNA damage sensing pathways can be activated by mechanical stress of the nucleus (31). DNA repair protein, XPC, which is involved in global genome nucleotide excision repair (GG-NER) by acting as a factor for damage sensing and DNA binding (32), was phosphorylated on serines 883 and 884 in cells treated with MAA. Another protein, RAD23B, which forms a

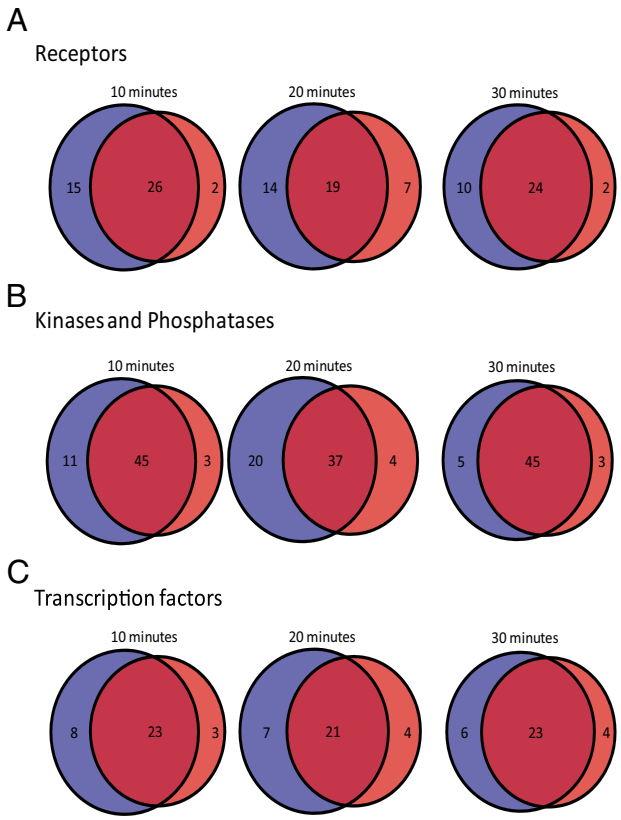

Fig. 4. Venn diagram showing the number of unique phosphorylated proteins (blue, MAA treatment; red, MM treatment) and overlapping phosphorylated proteins at different times, distinguished by protein function based on a manual screen of the protein lists: (*A*) receptors, (*B*) kinases and phosphatases, (*C*) transcription factors.

complex with XPC for GG-NER (33), was differentially modulated between the two biomaterials. MRE11, a protein in another DNA damage sensing complex, MRN complex, which senses double-stranded breaks in DNA, was phosphorylated in MAA-treated cells (34). These phosphorylation patterns suggest that there are differences in cell stress response to these two materials and that DNA damage signaling may play a role in the effects of MAA treatment, perhaps driving the change in cell sensitivity to apoptosis.

There were several transcription factors or transcription-associated proteins phosphorylated in the treated cells. Of interest is the transcription factor FoxO3, which was phosphorylated at S253 in MAA-treated cells; this phosphorylation is involved in angiogenesis (35) and in preventing apoptosis and cell cycle arrest (35). Another transcription factor, ATRX, is also phosphorylated with MAA treatment, which localizes it to the chromatin (36). Macrophages from ATRX-KO mice undergo apoptosis when stimulated with LPS and are more sensitive to DNA damage (37), again suggesting that MAA may affect the cell through DNA damage and apoptosis pathways that alter the transcriptome of the dTHP1 cells.

MS identification of phosphorylated proteins is an informative tool for biomaterial research, although not every pathway uses phosphorylation as a key step, nor is the function known for every phosphorylation site. Nonetheless, the results from this kind of screen point to an investigation into biological responses that might not have been immediately apparent. Clearly, the next step is to connect what we have learned here with a single model cell to the larger and more complex story of what happens in vivo and to learn why MAA materials, but not MM materials, generate a vascularized host response.

Discussion

This work demonstrated a method to identify interactions between materials and cells. Changes in phosphorylation patterns were characterized to identify biological processes that are differentially regulated in cells exposed to the two different biomaterials, MAA and MM. Rather than focusing on a particular pathway, the phosphopeptide TiO_2 enrichment-based MS approach was unbiased. Thus, previously unidentified interactions were identified, generating testable leads for the mechanism of interaction between materials and cells. The biological response of cells as they adapt to the biomaterial happens over several time scales: short-time morphological change, such as cytoskeleton rearrangement; intermediate-time scale changes in mRNA and protein expression; and the yet slower adaptation of cells, which is particularly dependent on transcription factor activity. The MS method identified signaling events for all these different types of cell response, even though the cells were stimulated for only 10–30 min, making this method a powerful tool to explore the initial interaction of materials with cells and tissues. This method of phosphoproteomic analysis will have profound impact on our understanding of how materials interact with cells and tissues. We expect that knowledge of these mechanisms of interaction will facilitate the development of new biomaterials for specific therapeutic applications.

Materials and Methods

Further details of materials and methods used in the present study are provided in *SI Materials and Methods*.

Polymer Synthesis. MAA or MM was copolymerized with IDA by using benzoyl peroxide as an initiator; copolymers were cast onto 22-mm-diameter glass coverslips from tetrahydrofuran (THF) solutions (13).

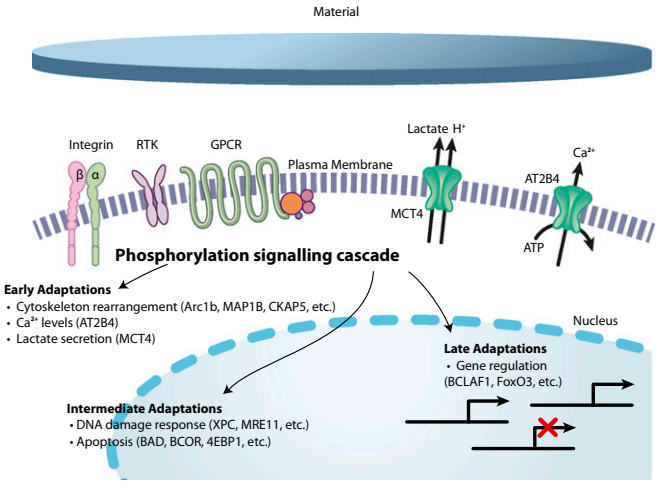

Fig. 5. Schematic illustration, based on the phosphosome, of some interactions of dTHP1 cells exposed to MAA or MM that potentially causes changes in the activation of surface receptors, such as integrins, receptor tyrosine kinase (RTK), and G protein-coupled receptors (GPCR). This causes changes in phosphorylation events of the downstream signaling cascades. This enables the cell to adapt to the new environment. Based on the particular data described here, early changes include cytoskeleton rearrangement and changes to calcium and lactate levels. Intermediate adaptations include changes in apoptosis and DNA damage response. Late adaptations are changes in gene regulation that involve transcription factors. Example proteins that are differentially phosphorylated between the two biomaterials are noted with each adaptation.

Cell Studies. THP1 cells were grown in suspension in RPMI medium supplemented with 10% (vol/vol) FBS, 25 mM Hepes, 2 mM L-glutamine, and 1% penicillin/streptomycin. The cells were differentiated into macrophages (i.e., dTHP1) with 100 nM phorbol 12-myristate 13-acetate (PMA) on six-well plate Transwell inserts made of polyethylene terephthalate with 0.4-μm pores (Corning). Cells were equilibrated in medium without PMA for 24 h, followed by serum starvation for 16 h to produce a cell population that was quiescent and homogenous; this reduced the variability of the subsequent peptide analyses.

Cells were exposed to 40% MAA or 40% MM for 10, 20, or 30 min by placing polymer-coated coverslips on top of the cell monolayer (Fig. 1*C*). After 10, 20, or 30 min, the coverslip and the medium were removed, the cells were quickly rinsed with PBS solution and lysed in 8-M urea containing phosphatase inhibitor mixture A (SC-45044; Santa Cruz Biotechnology).

Phosphopeptide Enrichment and MS Analysis. Phosphopeptides were enriched from the lysates by using a TiO_2 magnetic kit (Pierce) as previously described (14). Peptides were resuspended, desalted, and analyzed with an Orbitrap Velos mass spectrometer (Thermo Fisher Scientific) as previously described (14).

Raw data files (from MS) were submitted for database searching by using MaxQuant (version 1.3.0.5) under standard workflow and a modified UniProt/SwissProt protein database FASTA file. Peptide motifs were extracted from Motif-X (motif-x.med.harvard.edu) with at least 20 occurrences, 0.000001 significance, and International Protein Index (IPI) human proteome background. Further details are provided in *SI Materials and Methods*.

Data Analysis. The data were cleaned to remove random errors, such as identified nonphosphorylated peptides, and redundancies, by combining any equivalent peptides. Only the phosphorylated peptide sequences that were detected in at least two technical replicates were used in the analysis. The protein was considered to be phosphorylated if at least one peptide sequence in it was phosphorylated. For the analysis, only the presence of the phosphorylated peptide and protein, and not its intensity, was assessed.

The data analysis was performed on phosphorylated peptides and proteins. The differences in cells treated with MAA and MM copolymers were assessed across the three studied time points. A variety of targeted and bioinformatics approaches were taken to discern and characterize the temporal phosphorylation landscape for both biomaterials. The targeted screen of proteins was a manual approach to identify proteins of interest. The implications of the protein phosphorylation were assessed by cross-referencing phosphorylation of the proteins with the libraries of common signaling pathways listed on GeneCards (www.genecards.org) for a given protein, and the function of the phosphorylation was identified with the use of the phosphorylation site database Phosphosite Plus (www.phosphosite.org). Interesting hits were followed up with a literature review. In addition, biological implications of the phosphorylation cascades were assessed by identifying KEGG pathways using the DAVID Functional Annotation Tool (https://david.ncifcrf.gov/).

ACKNOWLEDGMENTS. This work was supported by the Natural Sciences and Engineering Research Council (NSERC), the Ontario Research Foundation, scholarships from the Province of Ontario (to A.L.) and the University of Toronto (to A.L.), the NSERC Collaborative Research and Training Experience Program (CREATE) in Manufacturing Materials (A.L.) and Mimetics (M3) training program (A.L.), a fellowship from the Canadian Institutes of Health Research (CIHR; to L.A.W.), and the CIHR Training Program in Regenerative Medicine (L.A.W.).

1. Brash JL (2000) Exploiting the current paradigm of blood-material interactions for the rational design of blood-compatible materials. *J Biomater Sci Polym Ed* 11(11): 1135–1146.
2. Stevens MM, George JH (2005) Exploring and engineering the cell surface interface. *Science* 310(5751):1135–1138.
3. Pashuck ET, Stevens MM (2012) Designing regenerative biomaterial therapies for the clinic. *Sci Transl Med* 4(160):160sr4.
4. Williams DF (2008) On the mechanisms of biocompatibility. *Biomaterials* 29(20): 2941–2953.
5. Bryers JD, Giachelli CM, Ratner BD (2012) Engineering biomaterials to integrate and heal: The biocompatibility paradigm shifts. *Biotechnol Bioeng* 109(8):1898–1911.
6. Chang DT, et al. (2008) Lymphocyte/macrophage interactions: Biomaterial surface-dependent cytokine, chemokine, and matrix protein production. *J Biomed Mater Res A* 87(3):676–687.
7. Engler AJ, Sen S, Sweeney HL, Discher DE (2006) Matrix elasticity directs stem cell lineage specification. *Cell* 126(4):677–689.
8. Keselowsky BG, Collard DM, García AJ (2005) Integrin binding specificity regulates biomaterial surface chemistry effects on cell differentiation. *Proc Natl Acad Sci USA* 102(17):5953–5957.
9. Eckhaus AA, Fish JS, Skarja G, Semple JL, Sefton MV (2008) A preliminary study of the effect of poly(methacrylic acid-co-methyl methacrylate) beads on angiogenesis in rodent skin grafts and the quality of the panniculus carnosus. *Plast Reconstr Surg* 122(5):1361–1370.
10. Martin DC, Semple JL, Sefton MV (2010) Poly(methacrylic acid-co-methyl methacrylate) beads promote vascularization and wound repair in diabetic mice. *J Biomed Mater Res A* 93(2):484–492.
11. Fitzpatrick LE, Chan JW, Sefton MV (2011) On the mechanism of poly(methacrylic acid -co-methyl methacrylate)-induced angiogenesis: Gene expression analysis of dTHP-1 cells. *Biomaterials* 32(34):8957–8967.
12. Fitzpatrick LE, Lisovsky A, Sefton MV (2012) The expression of sonic hedgehog in diabetic wounds following treatment with poly(methacrylic acid-co-methyl methacrylate) beads. *Biomaterials* 33(21):5297–5307.
13. Wells LA, Sefton MV (2014) The effect of methacrylic acid in smooth coatings on dTHP1 and HUVEC gene expression. *Biomater Sci* 2:1768–1778.
14. Guo H, et al. (2013) Integrative network analysis of signaling in human CD34(+) hematopoietic progenitor cells by global phosphoproteomic profiling using TiO2 enrichment combined with 2D LC-MS/MS and pathway mapping. *Proteomics* 13(8): 1325–1333.
15. Beltrao P, et al. (2009) Evolution of phosphoregulation: Comparison of phosphorylation patterns across yeast species. *PLoS Biol* 7(6):e1000134.
16. Weintz G, et al. (2010) The phosphoproteome of toll-like receptor-activated macrophages. *Mol Syst Biol* 6:371.
17. Huang W, Sherman BT, Lempicki RA (2009) Systematic and integrative analysis of large gene lists using DAVID bioinformatics resources. *Nat Protoc* 4(1):44–57.
18. Huang W, Sherman BT, Lempicki RA (2009) Bioinformatics enrichment tools: Paths toward the comprehensive functional analysis of large gene lists. *Nucleic Acids Res* 37(1):1–13.
19. Saito R, et al. (2012) A travel guide to Cytoscape plugins. *Nat Methods* 9(11):1069–1076.
20. Merico D, Isserlin R, Stueker O, Emili A, Bader GD (2010) Enrichment map: A network-based method for gene-set enrichment visualization and interpretation. *PLoS One* 5(11):e13984.
21. Halestrap AP, Wilson MC (2012) The monocarboxylate transporter family–role and regulation. *IUBMB Life* 64(2):109–119.
22. Welch MD, DePace AH, Verma S, Iwamatsu A, Mitchison TJ (1997) The human Arp2/3 complex is composed of evolutionarily conserved subunits and is localized to cellular regions of dynamic actin filament assembly. *J Cell Biol* 138(2):375–384.
23. Rueda D, et al. (2007) Bcl10 controls TCR- and FcgammaR-induced actin polymerization. *J Immunol* 178(7):4373–4384.
24. Yamashiro S, Yamakita Y, Ono S, Matsumura F (1998) Fascin, an actin-bundling protein, induces membrane protrusions and increases cell motility of epithelial cells. *Mol Biol Cell* 9(5):993–1006.
25. Schaller MD (2001) Paxillin: A focal adhesion-associated adaptor protein. *Oncogene* 20(44):6459–6472.
26. Desai S, Pillai P, Win-Piazza H, Acevedo-Duncan M (2011) PKC-ι promotes glioblastoma cell survival by phosphorylating and inhibiting BAD through a phosphatidylinositol 3-kinase pathway. *Biochim Biophys Acta* 1813(6):1190–1197.
27. Huynh KD, Fischle W, Verdin E, Bardwell VJ (2000) BCoR, a novel corepressor involved in BCL-6 repression. *Genes Dev* 14(14):1810–1823.
28. Kim ST, Lim DS, Canman CE, Kastan MB (1999) Substrate specificities and identification of putative substrates of ATM kinase family members. *J Biol Chem* 274(53): 37538–37543.
29. Yamagishi N, Ishihara K, Saito Y, Hatayama T (2006) Hsp105 family proteins suppress staurosporine-induced apoptosis by inhibiting the translocation of Bax to mitochondria in HeLa cells. *Exp Cell Res* 312(17):3215–3223.
30. Böck BC, et al. (2010) The PEA-15 protein regulates autophagy via activation of JNK. *J Biol Chem* 285(28):21644–21654.
31. Kumar A, et al. (2014) ATR mediates a checkpoint at the nuclear envelope in response to mechanical stress. *Cell* 158(3):633–646.
32. Sugasawa K, et al. (1998) Xeroderma pigmentosum group C protein complex is the initiator of global genome nucleotide excision repair. *Mol Cell* 2(2):223–232.
33. Chen L, Madura K (2006) Evidence for distinct functions for human DNA repair factors hHR23A and hHR23B. *FEBS Lett* 580(14):3401–3408.
34. Paull TT, Gellert M (1998) The 3′ to 5′exonuclease activity of Mre 11 facilitates repair of DNA double-strand breaks. *Mol Cell* 1(7):969–979.
35. Potente M, et al. (2005) Involvement of Foxo transcription factors in angiogenesis and postnatal neovascularization. *J Clin Invest* 115(9):2382–2392.
36. Bérubé NG, Smeenk CA, Picketts DJ (2000) Cell cycle-dependent phosphorylation of the ATRX protein correlates with changes in nuclear matrix and chromatin association. *Hum Mol Genet* 9(4):539–547.
37. Conte D, et al. (2012) Loss of Atrx sensitizes cells to DNA damaging agents through p53-mediated death pathways. *PLoS One* 7(12):e52167.